Rationalization of the mechanism of in situ Pd(0) formation for cross-coupling reactions from novel unsymmetrical pincer palladacycles using DFT calculations

Article (Accepted Version)

Rationalization of the Mechanism of *in situ* Pd(0) Formation for Cross-Coupling Reactions from Novel Unsymmetrical Pincer Palladacycles Using DFT Calculations

Sarote Boonseng, Gavin W. Roffe, Msugh Targema, John Spencer,* Hazel Cox*

Department of Chemistry, School of Life Sciences, University of Sussex, Falmer, Brighton, East Sussex, BN1 9QJ, UK

Abstract

Density functional theory (DFT) is used to determine the mechanism for Pd(0) generation from pincer palladacycle pre-catalysts. The elucidated mechanisms comprise two key steps, transmetallation and reductive elimination. It is found that the presence of a base in the pre-catalyst activation step serves to significantly lower the Gibbs free energy barrier of the transmetallation step and the Gibbs free energy of the overall pre-catalyst activation. The DFT results are used to rationalize the catalytic activity of a number of pincer palladacycles in the Suzuki-Miyaura coupling of sterically demanding and electronically deactivated aryl bromides with 2-tolyboronic acid. A strong correlation exists between the Gibbs free energy barrier of the transmetallation step and/or overall pre-catalyst activation energy and the percentage conversions of the Suzuki- Miyaura coupling in the presence of the novel pre-catalysts. The data presented suggest that the slow, controlled release of the "true, active catalyst," Pd(0), from the pincer palladacycle pre-catalysts provides the optimum reaction conditions and may be achieved by a high transmetallation energy barrier or overall pre-catalyst activation energy or both.

1. Introduction

The numerous application of palladacycles [1] in catalysis [2–4] since the discovery of their catalytic activity by Hermann and Beller *et al*., [5,6] over the last two decades cannot be overemphasized. This has become a vibrant research area amongst academics and industrialists as evidenced by the plethora of scholarly articles and reviews [1–4] and an excellent book [7] is now available. Of increasing significance is the employment of these species, especially the pincer-type palladacycles (in which a Pd-C bond is intra-molecularly stabilized by two donor atoms in a YCY'

architecture, where C is the carbon of the Pd-C bond [8–11]) in the Suzuki-Miyaura [12,13] (SM) and Mizoroki-Heck [14] carbon-carbon (C-C) cross-coupling reactions which have emerged as highly important and facile routes to e.g., complex pharmaceuticals and industrially important starting materials [7]. Symmetrical palladacycles are attractive [1] due to their relative ease of synthesis as compared to unsymmetrical analogues. However, the latter offer the potential for fine tuning their reactivity and properties by adapting their ligand architectures [13].

Moreover, a number of reports in the literature assert that unsymmetrical pincer palladacycles often exhibit higher catalytic activity than their symmetrical counterparts [13,15,16]. In all cases, palladacycles, whether symmetrical, unsymmetrical pincers, or of the type C-Pd-Y, are thought to be pre-catalysts and, hence, precursors to Pd(0) [5,6,17–23] (**Scheme 1** and **2**).

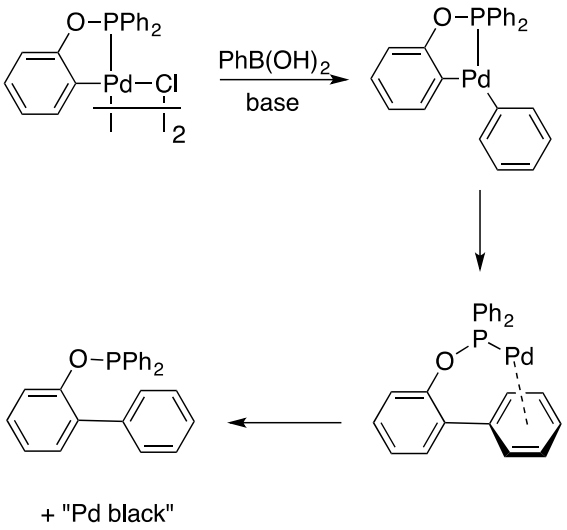

Scheme 1. Stabilization of Pd(0) in C-Pd-Y palladacycles.

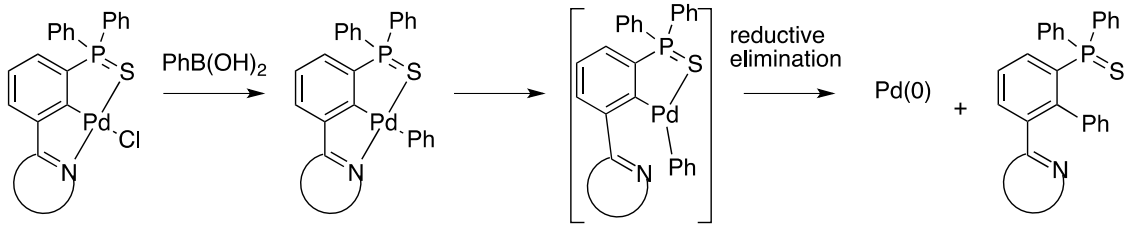

Scheme 2. Formation of Pd(0) from unsymmetrical pincer palladacycles.

In Palladacycle chemistry, the well-studied key steps that occur during the SM reactions namely, transmetallation (TM) and reductive elimination (RE), have been

studied via experimental [21] and theoretical (density functional theory, DFT) investigations [24].

Herein, we present a study of the pre-catalyst activation process for SM reactions involving palladacycles. The investigation starts with a thorough exploration of the formation of Pd(0) from symmetric pincer palladacycles, YCY (**1** – **3**, **Fig. 1**) with and without base, and with and without solvent effects. This is extended to model unsymmetrical pincer YCY' palladacycles (**4** – **6**, **Fig. 1**) to determine the effect of different donor ligand groups on the process. Based on the conclusions from these extensive studies on small and/or model systems, the formation mechanism of Pd(0) from recently synthesized YCY' pincer palladacycles (**7** – **12**, **Fig. 1**) will be explored. Finally, the results of these theoretical investigations will be used to rationalize catalytic testing of the newly-synthesized pincer palladacycles (**7** – **12**, **Fig. 1**) in the SM coupling of sterically demanding and electronically deactivated aryl bromides with phenylboronic acid. The synthesis has been reported for: **1** [25–27], **2** [28], **7a** [29], **7b-f** [30] and **8-11** [31].

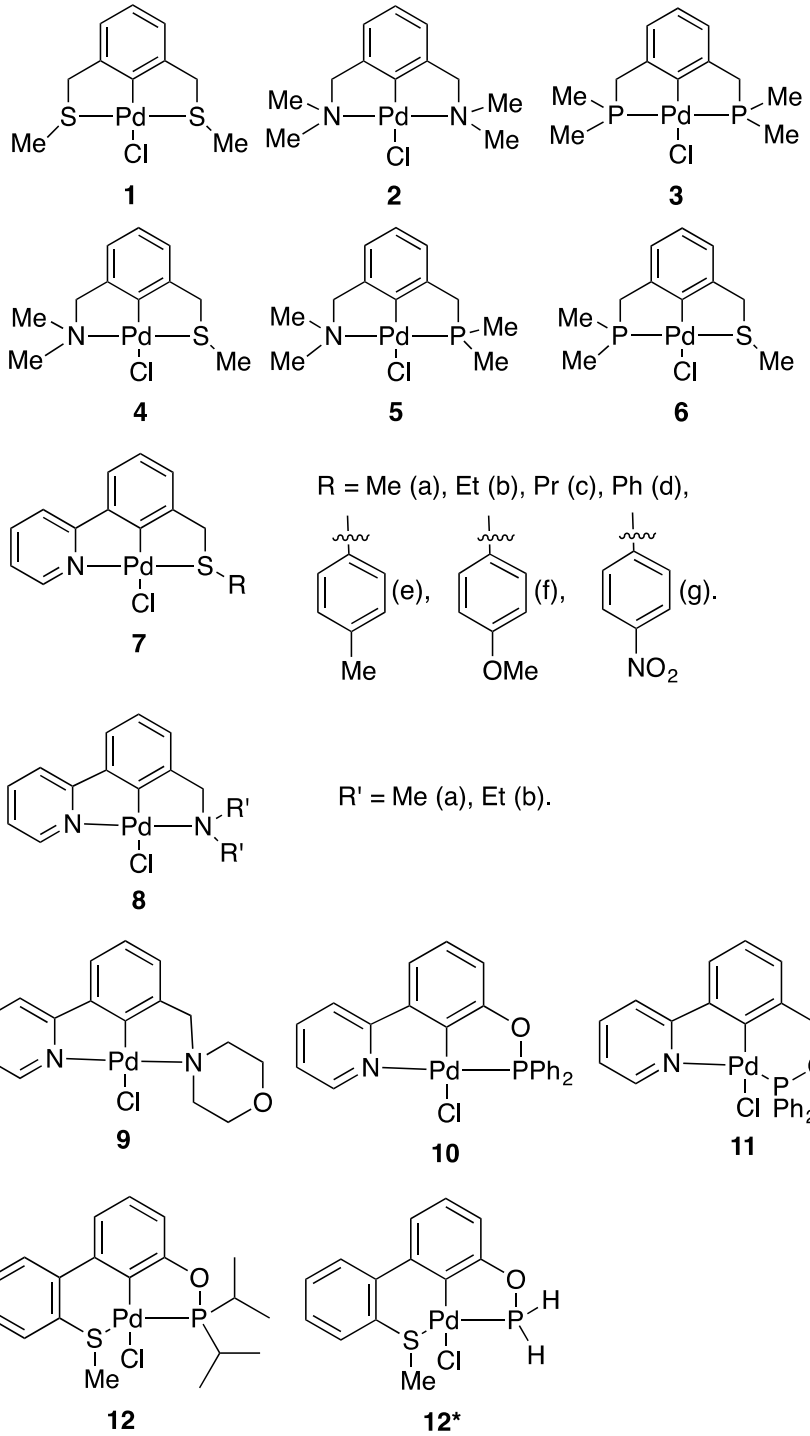

Fig. 1. Pincer palladacycles investigated in this study.

2. Computational Details

Calculations were performed using density functional theory as implemented in the GAUSSIAN 09 [32] package. All Pd complexes along the reaction pathway were considered in their singlet spin state. It was shown previously [9] that the geometric features of pincer palladacycles can be accurately reproduced by both PBE [33–35]

and ωB97XD [36], and that the ωB97XD functional provides accurate energetics due to the inclusion of dispersion and long range corrections [37]. The detailed study of **1 - 6**, along with **7a**, was performed at the ωB97XD/6-311++G(2df,2p)[SDD]//PBE/6-31+G(d,p)[SDD] level of theory, and investigation of the recently synthesized pincer palladacycles (**7a-g - 12**) was performed at the ωB97XD/6-311++G(2df,2p)[SDD]//ωB97XD/6-31++G(d,p)[SDD] level of theory. Here the notation, 6-31+G(d,p)[SDD] for example, implies all non-metal atoms were described by the standard basis set: 6-31+G(d,p) in this case, and palladium was described by the relativistic effective core potential, SDD [38,39].

In each case, the minima and transition states on the potential energy surface (PES) were confirmed by the absence or presence of a single imaginary vibrational frequency mode, respectively [40] via frequency calculations performed at 298.15 K and 1 atm. The connectivity of the transition states to their adjacent minima was confirmed by eigenvector following calculations [41–43]. The Gibbs free energy corrections obtained at PBE/6-31+G(d,p)[SDD] or ωB97XD/6-31++G(d,p)[SDD] level of theory were applied, un-scaled, to the single point energy calculations using ωB97XD/6-311++G(2df,2p)[SDD].

Solvent effects were included using the polarizable continuum model (PCM) [44,45] with the continuous surface charge formalism of Scalmani and Frisch [46]. Solvent corrections were obtained for the gas-phase optimized geometries using the self-consistent reaction field (SCRF) with Universal Force Field (UFF) atomic radii at the ωB97XD/6-311++G(2df,2p)[SDD] level of theory. For **1**-**6** the non-polar solvents toluene (ε = 2.374), tetrahydrofuran (ε = 7.426) and the polar solvent acetonitrile (ε = 35.688) were investigated. However, after this initial study was performed it was found that, experimentally, *o*-xylene was the solvent of choice, and so for **7a**-**12** *o*-xylene (ε = 2.545) and acetonitrile (ε = 35.688) were investigated. For comparison purposes, **7a** was calculated with all four solvents for the mechanism without base.

A topological analysis of the electron density was performed using Bader's Quantum Theory of Atoms in Molecules (QTAIM) [47] method as implemented in the Multiwfn program [48]. In doing this, the ωB97XD level of theory was employed and the ECP was replaced with an all electron basis set, DGDZVP [49] to generate the wavefunction and hence, obtain reliable QTAIM parameters, i.e., the ωB97XD/6-311++G(2df,2p)[DGDZVP] level of theory was used.

3. Results and Discussion

The formation of Pd(0), believed to occur prior to catalysis in SM cross-coupling reactions employing palladacycles [22,23,50], was investigated by considering the reaction of each pincer palladacycle with phenylboronic acid (**Scheme 3**).

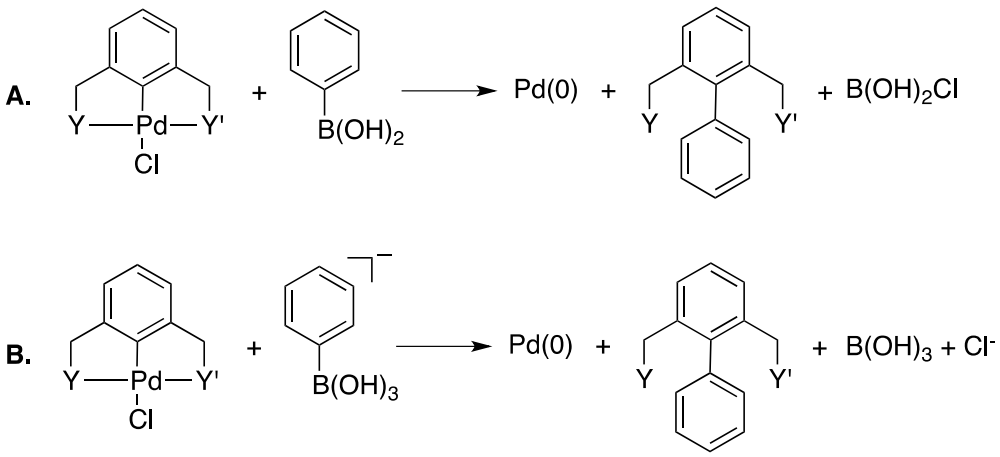

Scheme 3. Formation of Pd(0) from the reaction of pincer palladacycles and phenylboronic acid; **A**. without base and **B**. with base.

3.1. Pd(0) formation from pincer palladacycles

3.1.1. Base-free formation of Pd(0) from symmetrical pincer palladacycles

A proposed general mechanism of Pd(0) formation from **1**-**3** based on **Scheme 3A** is presented in **Scheme 4** and the reaction energy profiles are presented in **Fig. 2**. The Pd(0) formation mechanism from the symmetrical pincer complexes begins with the non-covalent interaction between the pincer and the phenylboronic species leading to the stabilization and orientation [51–53] of intermediate one (**Int1A**) from **3** (PCP) while that from **1** (SCS) and **2** (NCN) are slightly destabilized relative to the reactants.

The transmetallation (TM) step which involves the cleavage of the halide ligand from the Pd(II) centre as the organic moiety (aryl ring) is transferred to the Pd(II) centre from boron, occurs via a concerted four-centered transition state [54,55], **TS1-2A**, with an energy barrier of 208.8, 202.2 and 289.4 kJ mol^{-1} respectively for **1**, **2** and **3**. These energy barriers are in close agreement with literature precedents for the TM step of the SM reactions in the gas-phase without base [56]. The significantly larger TM energy barrier **TS1-2A** involving **3** (PCP) may be attributed to the stabilizing σ-donating and π-accepting character [9,57] of phosphines which results in stronger

dative bonding and a greater covalent character in the Pd-P bond compared with Pd-S and Pd-N [9]. The cleaved halide binds to the resulting electron deficient boron species to form the boric chloride, which separates from the TM product in **Int3A**. In **Int2A** and **Int3A** the symmetrical pincer complexes has one of the side arms de-coordinated.

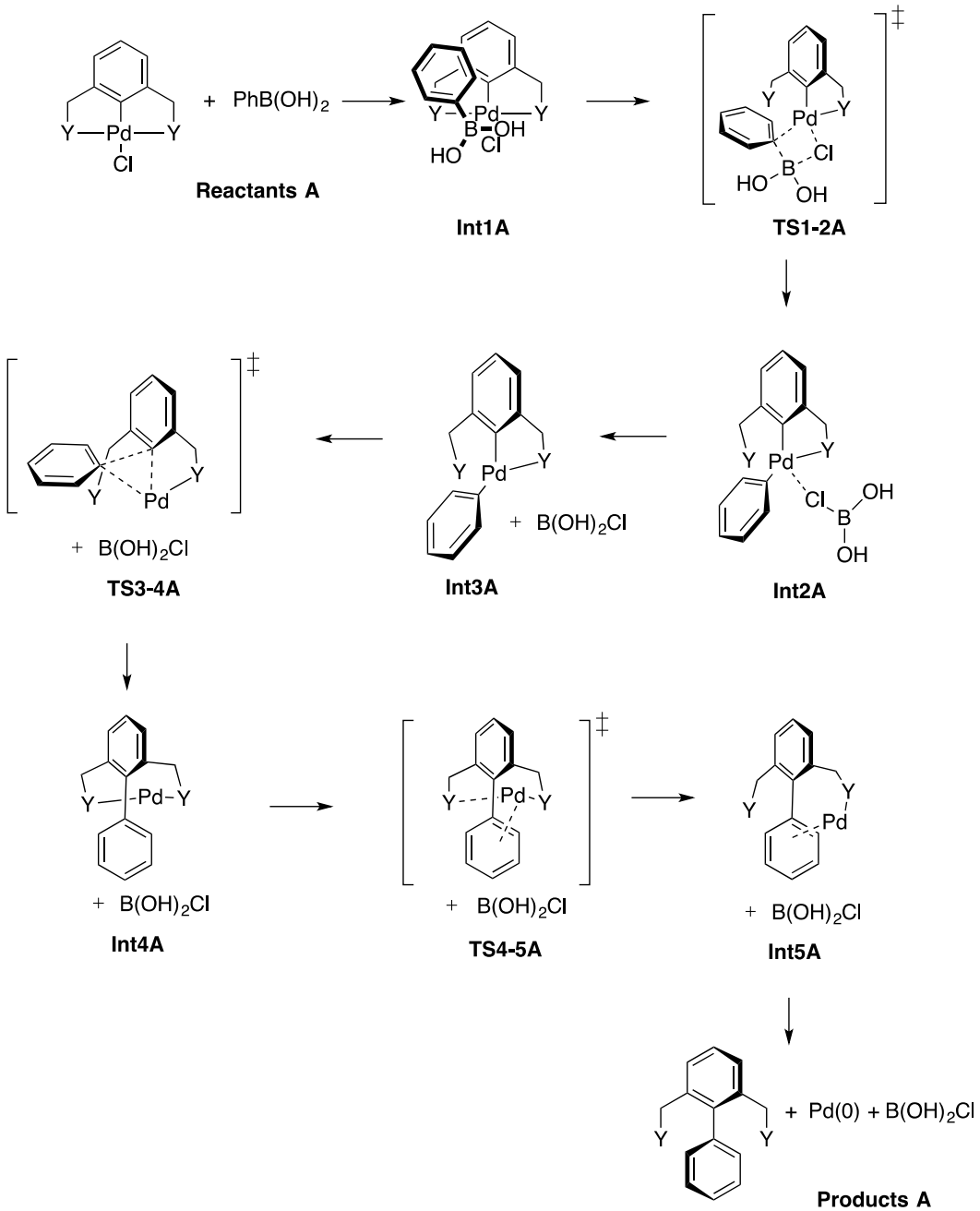

Scheme 4. Proposed general mechanism of the base-free Pd(0) formation from symmetrical pincer palladacycles.

The reductive elimination (RE) step involves a low energy, three-centered dissociative transition state [58,59], located at 238.5, 250.0 and 282.1 kJ mol^{-1} (from

1-3 respectively) above the reactants. In this step, the two Pd-C bonds are broken to form the new C-C bond. This is the step that reduces the Pd(II) centre in the pincers to the Pd(0) to be released as the catalyst needed for catalysis in cross-coupling reactions [22,23]. In the case of **1** and **3** the RE step leads to the re-coordination of the previously de-coordinated side arm in **Int4A** located at 65.8 and 66.6 kJ mol^{-1} above the reactants (for **1** and **3** respectively) before proceeding to **Int5A** via **TS4-5A** which involves a second de-coordination step of one of the stabilizing side arms preparatory to the release of the reduced metal for catalysis. However, in the case of **2** (NCN) **Int5A** results directly from the RE transition state. **Int5A** is located at 52.3, 87.0 and 108.6 kJ mol^{-1} above the reactants in the reaction of **1-3**, respectively [60].

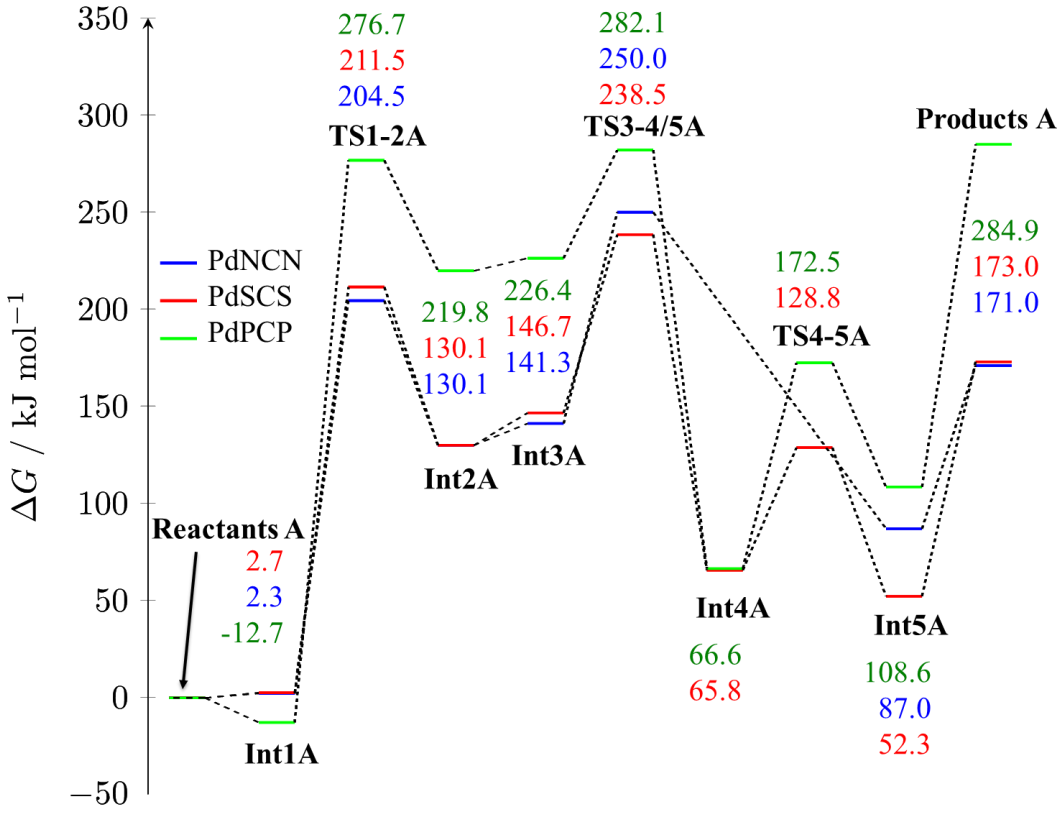

Fig. 2. The gas-phase Gibbs free energy profiles for the Pd(0) formation reaction of **1-3** in the absence of base (**Scheme 4**) obtained at the ωB97XD/6-311++G(2df,2p)[SDD]//PBE/6-31+G(d,p)[SDD] level of theory.

In summary, the overall reaction leading to the formation of the active catalyst from symmetrical pincer palladacycles is found to be endergonic with an overall energetic cost of 173.0, 171.0 and 284.9 kJ mol^{-1}, for **1** (SCS), **2** (NCN) and **3** (PCP), respectively. It is found that the TM step has the largest energy barrier indicating that this is the rate-determining step of the pre-catalyst activation process of **1-3** resulting

from **Scheme 3A**. Therefore, the reaction will more readily occur for **2** and **1** when compared to **3** for the reaction shown in **Scheme 3A**.

3.1.2. Formation of Pd(0) from symmetrical pincer palladacycles in the presence of a base

The proposed general mechanism of Pd(0) formation from **1-3** based on **Scheme 3B** is presented in **Scheme 5**.

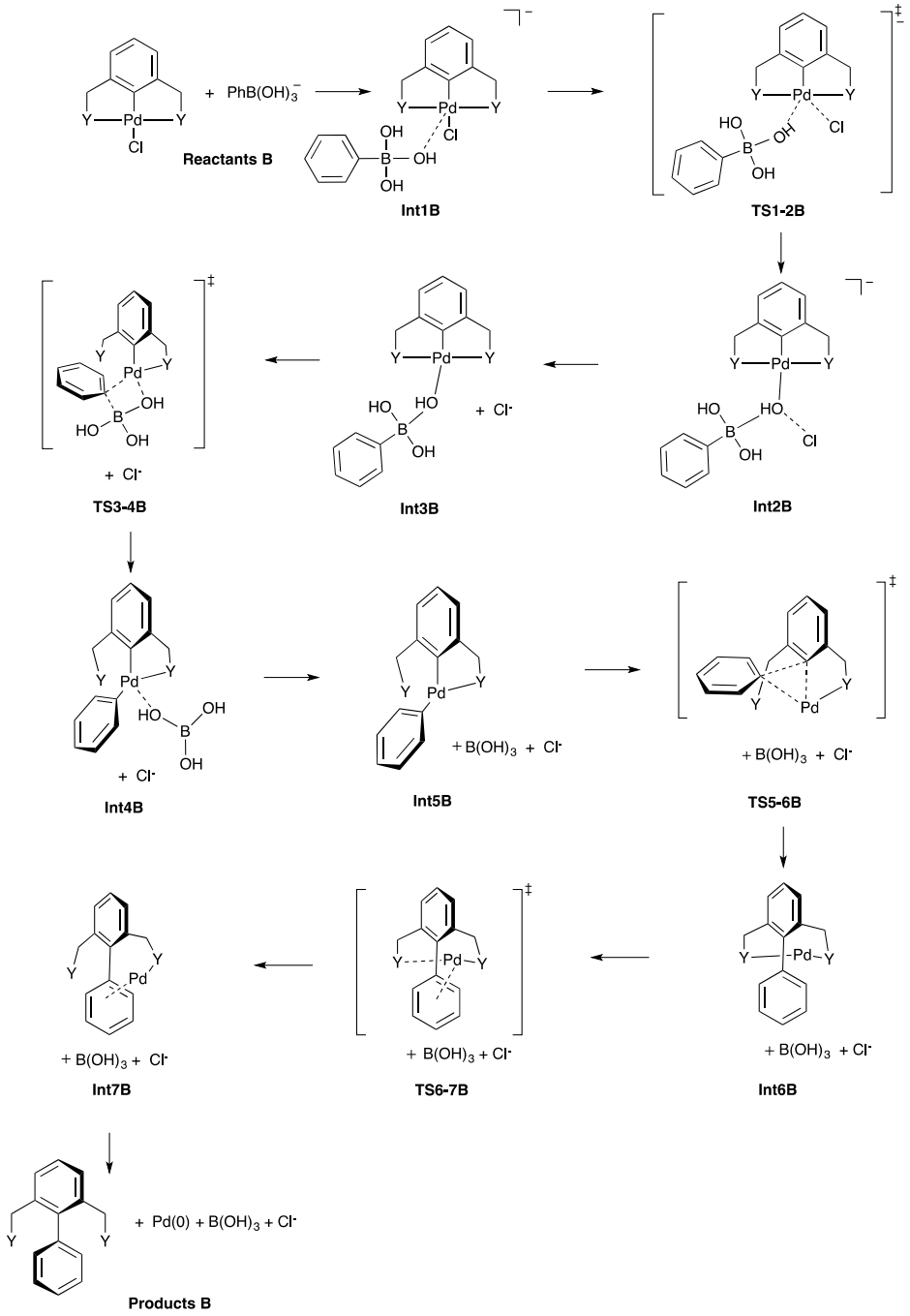

Scheme 5. Proposed general mechanism of Pd(0) formation from symmetrical pincer palladacycles in the presence of a base.

A widely reported role of the base in SM reactions is to attack the phenylboronic acid to form the boronate species ($R\text{-}B(OH)_3^-$) [56,61,62], which then goes into the reaction as the nucleophile in place of the phenylboronic acid as illustrated. The Pd(0) formation reaction begins with a weak intermolecular interaction of the reacting species leading to **Int1B**. Except for the interaction of **1** (SCS) for which **Int1B** is slightly destabilized, the intermediate is stabilized, (and to a similar extent: 29 and 27 $kJmol^{-1}$ for **2** (NCN) and **3** (PCP), respectively). A possible explanation for this occurrence in **Int1B** for **2** and **3** is the greater hydrogen bonding interactions of the boronate species with the donor ligands. This is evidenced by the number of bond paths and bond critical points (BCPs) in the molecular graph of the intermediate from the result of its QTAIM analysis (see Supplementary information). The next step of the reaction is the removal of the halide ligand from the Pd(II) coordination sphere via a substitution nucleophilic bimolecular (S_N2) step, **TS1-2B** to generate **Int2B** with a Pd-O bond. **TS1-2B** has a low energy barrier of 10.6, 31.6 and 28.5 kJ mol^{-1} for the reaction involving **1**, **2** and **3** respectively. **Int2B** transforms to **Int3B** by a barrier-less rearrangement of the borate in the Pd(II) co-ordination sphere.

The TM step via **TS3-4B**, and the RE step via **TS5-6B**, and the remaining steps of the Pd(0) formation process essentially follow the same mechanism as the base-free reaction, including the additional re-coordination of the previously de-coordinated side arm in **Int6B** in the case of the mechanism for **1** and **3**, and the absence of this step for the mechanism of **2** (NCN) where **Int7B** results directly from the RE transition state, as depicted in **Fig. 3**.

However, the TM energy barrier for this mechanism has an energy barrier of 93.5, 105.5 and 162.0 kJ mol^{-1} for the reaction of **1**, **2** and **3**, respectively. This is a significantly lower energy barrier for the TM step compared to the base-free mechanism discussed in *3.1.1*.

Although the energies relative to the reactants differ significantly, the RE energy barrier for the reaction of **1** (SCS), **2** (NCN) and **3** (PCP), respectively, is 91.8, 108.6 and 55.7 $kJmol^{-1}$ (**Fig. 3**) and is almost identical to the base-free values of 91.8, 108.7, and 55.7 $kJmol^{-1}$ (**Fig. 2**). The energy barriers of the RE step obtained in this work are similar to those previously reported for the same step of C-C cross-coupling reactions [63,64].

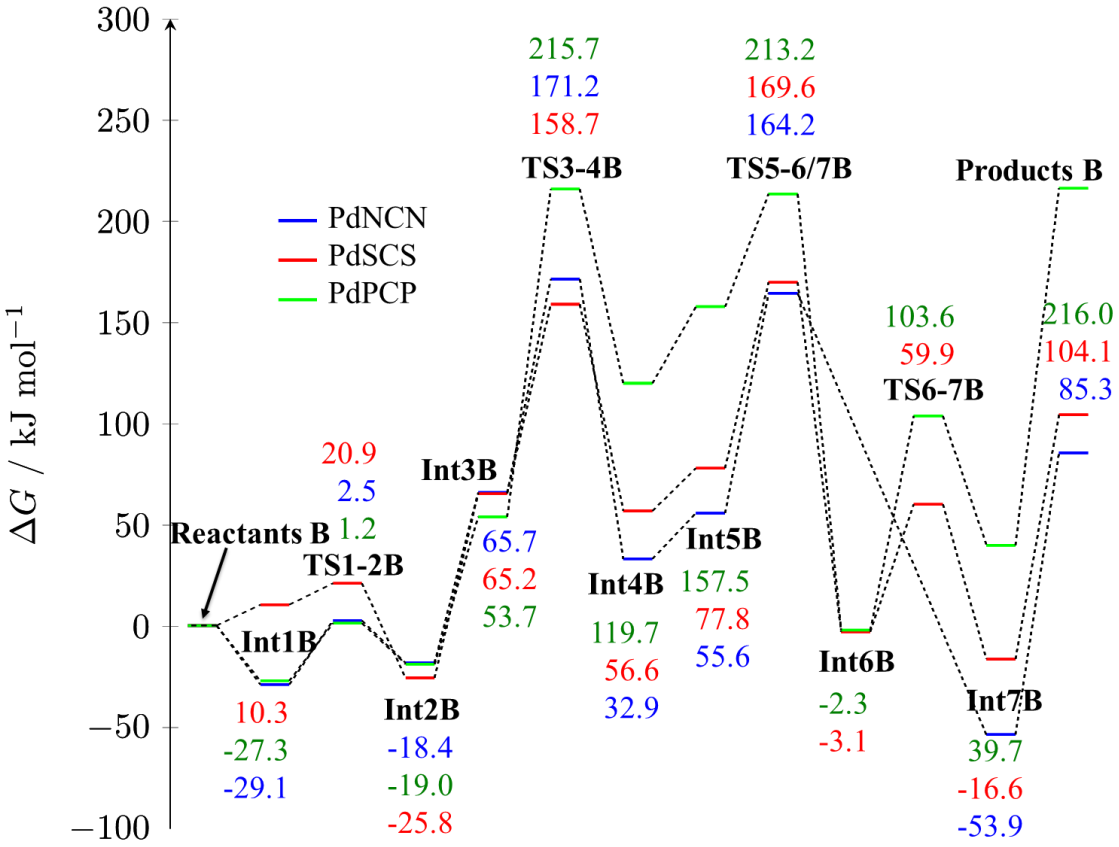

Fig. 3. The gas-phase Gibbs free energy diagrams for the Pd(0) formation reaction of **1-3** in the presence of base (**Scheme 5**) obtained at the ωB97XD/6-311++G(2df,2p)[SDD]//PBE/6-31+G(d,p)[SDD] level of theory.

Similarly, the energy barriers for the last step, **TS6-7B** before the release of the catalyst from **1** and **3**, 63.0 and 105.9 kJ mol^{-1} respectively are identical to the values for the barrier to **TS4-5A** for the base-free mechanism discussed in *3.1.1*.

In summary, the preceding discussion reveals that the primary role of the base in the reaction is to significantly lower the energy barrier of the TM step to enable the Pd(0) formation from the pincers to be initiated more readily at a lower thermodynamic cost. This effect of the base on the TM step of SM reactions has been reported previously in the literature [56,61,62]. Furthermore, the TM energy barrier is now of a similar magnitude to the barrier for RE. Additionally, although the process is still endergonic, the overall reaction energy has decreased from 173.0, 171.0 and 284.9 kJ mol^{-1} in the absence of base to 104.1, 85.3, and 216.0 kJ mol^{-1} in the presence of base for reactions of **1**, **2** and **3**, respectively.

3.1.3. Formation of Pd(0) from model unsymmetrical pincer palladacycles, with and without base

The unsymmetrical pincer palladacycles, YCY', **4 - 6**, **Fig. 1**, were investigated to determine the role and/or effect of the donor ligands on the reaction mechanisms in **Scheme 3A** and **3B**. The full schemes and energy profiles are provided in the Supplementary Information. As discussed in Section *3.1.1* the base-free mechanism (**Scheme 4**) involves de-coordination of a donor ligand arm from Pd(II) to facilitate transmetallation and reductive elimination. In the case of an unsymmetrical pincer palladacycle, where Y ≠ Y', either arm can potentially de-coordinate from the Pd(II) centre in the TM step of the mechanism based on **Scheme 3A**, each leading to the active catalyst following the same mechanism discussed in the previous sections. For **4** and **5** this was the case, but for **6** (PCS) only the reaction involving sulfur de-coordination from the Pd(II) centre was found. In the case of the base-free reaction mechanism for **5** (PCN), an additional step was required when the phosphine arm of the pincer de-coordinated from the Pd(II) centered in the TM step. This then involved a re-coordination of the phosphine arm via a rotational barrier, which leads to the same intermediate as that which results from the mechanism involving the other arm of the complex de-coordinating first.

Furthermore, when the pincer palladacycle has a S or P containing group, an additional de-coordination step occurs after the RE step (as previously for **1** (SCS) and **3** (PCP) via **TS4-5A**) which also leads to two routes depending on whether Y or Y' is involved in the second de-coordination step prior to the release of the reduced metal for catalysis. In all cases, the key features of Pd(0) formation from the pincers remains the same as that discussed in *3.1.1*. The energy profile for **4** (SCN) is provided in **Fig. 4**.

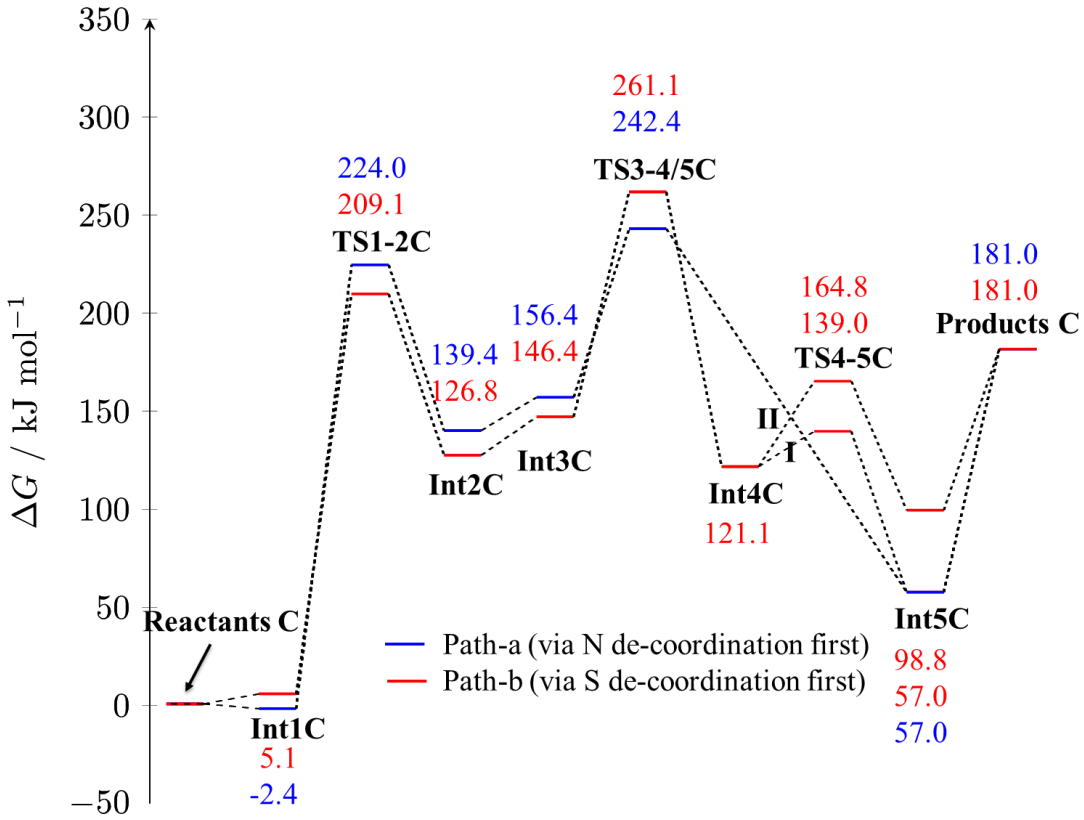

Fig. 4. The gas-phase Gibbs free energy profiles for the base-free Pd(0) formation reaction of **4** (SCN) at the ωB97XD/6-311++G(2df,2p)[SDD]//PBE/6-31+G(d,p)[SDD] level of theory. Path-a = N de-coordinates first from Pd at TM, Path-b = S de-coordinates first from Pd at TM, route **I** = N de-coordinates first from Pd and route **II** = S de-coordinates first from Pd.

In the case of the mechanism of Pd(0) formation based on **Scheme 3B** only one side arm was found to de-coordinate in the TM step prior to the RE step and remained de-coordinated through the remaining key steps of the process. In each case the stronger Pd-Y bond remained coordinated, i.e., Pd-P in the case of **5** (PCN) and **6** (PCS), and Pd-S in case of **4** (SCN) [30].

In summary, the elucidated Pd(0) formation mechanisms from the previously reported, **1** and **2**, and model, **3** - **6**, simple pincer palladacycles indicate that the mechanism involves two key steps, TM and RE. For all the elucidated routes, the TM is most probably the rate-determining step based on its activation energy barrier compared to that for the RE step. From the reaction energy profiles of the respective pincers, **1** - **6**, obtained with and without base, it is observed that the primary role of the base in the process is to significantly lower both the energy barrier of the TM step and the overall Gibbs free energy of reaction for easy release of the requisite Pd(0) catalyst for SM coupling reactions. Furthermore, for all the unsymmetrical pincer

complexes, only one route is obtained in the presence of a base prior to TM, contrary to the base-free mechanism.

3.1.4. Solvation effects on the Pd(0) formation pathways

The effect of solvation on the generation of Pd(0) from the pincer complexes **1** – **6** has been investigated using the PCM model with the non-polar solvents: toluene (ε = 2.374) and tetrahydrofuran (ε = 7.426), and the polar solvent acetonitrile (ε = 35.688). **Table 1** presents the solvent-corrected TM and RE energy barrier ($\Delta G^{\ddagger}$) and the overall Gibbs free energy of reaction (ΔG_r) of the Pd(0) formation process for **1** which is indicative of the trend for all palladacycles **1** – **6**.

Table 1. The Gibbs free energy barriers, $\Delta G^{\ddagger}$ for the TM and RE steps, and the Gibbs free energy of reaction, ΔG_r (in kJ mol^{-1}) for **1** (SCS) without base (**Scheme 3A**) and with base (**Scheme 3B**) in solvent.

PdSCS	Step	Gas Phase	Solvent		
			Toluene	THF	Acetonitrile
Base-free	TM	208.8	217.3	223.2	226.0
	RE	91.8	98.9	105.5	109.3
	ΔG_r	**173.0**	**186.7**	**197.7**	**203.0**
With base	TM	93.5	98.7	103.1	105.2
	RE	91.8	98.8	105.4	109.3
	ΔG_r	**104.1**	**57.1**	**39.8**	**35.1**

The solvent-corrected energy calculated at each stationary point along each of the reaction profiles is provided in the Supplementary Information. It can be seen in **Table 1** that the effect of the solvent correction on both the reaction barriers ($\Delta G^{\ddagger}$ of TM, RE) and the base-free reaction energy (ΔG_r for the reaction) is to increase the energy, making the reaction slightly less favorable. The solvent correction increases marginally as the applied solvent static dielectric constant is increased.

In the presence of base, the trends in the reaction barriers follow a similar pattern, however, the reaction energy (ΔG_r) decreases with increasing solvent field (**Table 1**) and the energies vary significantly with the applied solvent field. This is attributed to the stabilization of the free halide ligand, and hence the reaction, by the solvent. It is clear from this analysis that the inclusion of solvent effects is crucial when considering the mechanism with base.

A summary of the activation energy barriers for the TM and the RE and the overall reaction energies of **1 - 6** leading to Pd(0) formation for catalysis in the SM coupling

reactions including solvent corrections (toluene and acetonitrile) in the presence of base is presented in **Table 2**. Also included for comparison are the TM and RE energy barrier and the overall reaction energy of **7a** with solvent the corrections using *o*-xylene and acetonitrile.

Table 2. The $\Delta G^{\ddagger}$ for TM, RE and ΔG_r (in kJ mol^{-1}) of the Pd(0) formation reaction of **1**-**6** obtained at the ωB97XD/6-311++G(2df,2p)[SDD]//PBE/6-31+G(d,p)[SDD] level of theory and **7a** obtained at the ωB97XD/6-311++G(2df,2p)[SDD]//ωB97XD/6-31++G(d,p)[SDD] level of theory with solvent corrections (in toluene and acetonitrile) in the presence of a base.

Pincer	$\Delta G^{\ddagger}$ (TM)		$\Delta G^{\ddagger}$ (RE)		ΔG_r	
Complex	Toluene	Acetonitrile	Toluene	Acetonitrile	Toluene	Acetonitrile
1 SCS	98.7	105.2	98.8	109.3	57.1	35.1
2 NCN	107.9	106.0	114.7	125.1	43.6	29.4
3 PCP	163.1	163.7	62.3	70.6	169.4	147.2
4 SCN	122.3	117.5	91.9	101.0	52.8	37.8
5 PCN	127.9	124.7	85.4	96.0	124.2	109.8
6 PCS	119.0	114.1	89.9	102.5	110.9	97.2
7a SCN	99.7*	102.4	95.4*	103.3	71.6*	53.9

* Solvent correction in *o*-xylene

3.2. Formation of Pd(0) from novel unsymmetrical pincer palladacycles for SM coupling reactions

Based on the analysis presented in the previous sections, it can be concluded that the presence of base and the inclusion of solvent effects have a significant effect on the energetics of the reaction mechanism for the formation of Pd(0) from palladacycles.

In this section, the formation of Pd(0) from the recently synthesized pincer palladacycles **7** – **12** is considered. Only the mechanism with base (**Scheme 3B**) is investigated (with the exception of **7a** for which both mechanisms were considered, see Supplementary Information) and solvent corrections are included using the PCM model with the solvent *o*-xylene (ε = 2.545), which has a similar dielectric constant to toluene (ε = 2.374) and was used in the experimental section to follow, and acetonitrile (ε = 35.688). Due to the increasing steric demand in **7** – **12**, the geometries of **7** – **11** and **12*** (where **12*** is **12** with ^{i}Pr groups replaced with H) were optimized using the ωB97XD exchange-correlation functional as discussed in the computational details.

The optimized structures, depicting the stereo-chemistry for the formation of Pd(0) from **7a** is provided in **Fig. 5**. The key transition states and important intermediates are representative of those obtained in all the pathways with base.

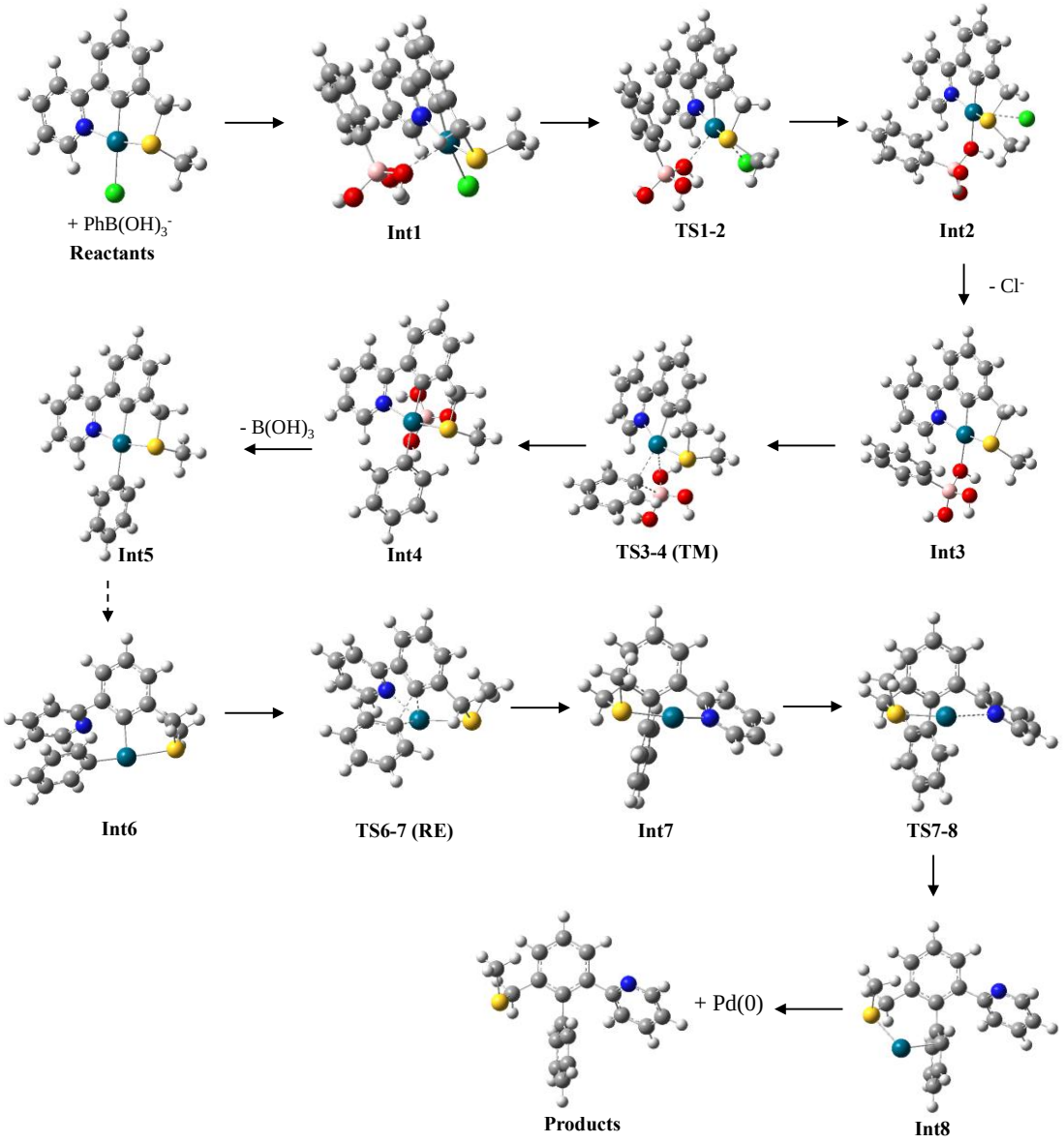

Fig. 5. The geometry-optimized structures obtained along the reaction mechanism pathway for Pd(0) formation from **7a** in the presence of a base. The pathway follows in essence **Scheme 5** but contains an addition step **Int 5** to **Int 6** (via a transition state not calculated).

The mechanism follows in essence **Scheme 5**, however the product of the TM step does not have a de-coordinated side arm (see **Int4**, **Fig. 5**). Nevertheless, it does go through a de-coordination step prior to the RE to obtain (see **Int6**, **Fig. 5**, which corresponds to the **Int5** structure in **Scheme 5**). A summary of the TM and RE energy

barriers and overall reaction energies (solvent corrected using *o*-xylene) are presented in **Table 3** and discussed in the context of the experimental catalytic activity in the next section.

3.3. Rationalization of the catalytic activity of the newly synthesized unsymmetrical pincer palladacycles

The catalytic activity in the SM coupling reaction of some of the recently synthesized unsymmetrical pincer palladacycles, **7-12**, was examined using the pincers as the pre-catalysts. The pincer complexes investigated here were **7a-c**,**e**,**f** and **8b-12** (Table 3).

3.3.1. Effect of asymmetry on the catalytic activity of palladacycles

A summary of the catalysis results is shown in **Table 3**. Also in **Table 3** is the catalytic activity of previously reported palladacycles: a symmetrical NCN pincer palladacycle **14** [65], a symmetrical SCS pincer palladacycle **15** [25] and the Herrmann-Beller palladacycle **16** [5,6] to provide a comparison of the present data with symmetrical pincer palladacycles (structures presented in **Fig. 6**).

The results collectively show that amongst the novel pre-catalysts, the N'CN and PCN (i.e., **8b** - **11**) pincer palladacycles achieve the highest % conversions of the reacting species while the SCN (**7a-c**, **7e** and **7f**) pincers achieve the lowest GC conversions. The single PCS (**12**) pincer complex is found to have intermediate catalytic activity between the highest and lowest. The data in **Table 3** reveal that the transmetallation and reductive elimination energy barriers of the N'CN pincer palladacycles (**8b** and **9**) are larger than those of the SCN pincer palladacycles, resulting in the much higher catalytic activity.

A striking feature of the data presented in **Table 3** is the higher overall reaction energy (ΔG_r) for the PCN (**10** and **11**) pincer palladacycles. It is likely that this is a significant factor in the high catalytic activity exhibited by the PCN pincer palladacycles. This is possibly the reason for the longevity of phosphinite palladacycles [18,19] and hence their high catalytic activity. The transmetallation barrier for the PCN pincer palladacycle **10** on the other hand, is similar to the SCN palladacycles tested in this study.

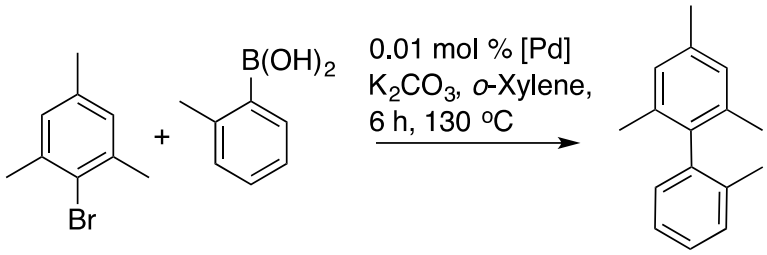

13

Table 3. Catalytic activity of the pincer complexes **7 - 12** compared to the calculated TM, RE barrier and overall reaction energy (kJ mol^{-1}) elucidated for their Pd(0) formation. Also presented are the literature data for three symmetrical pincer palladacycles, **14** – **16** (see **Fig. 6** for details).

PdYCY'	**Y**	**Y'**	$\Delta G^{\ddagger}$(TM)	$\Delta G^{\ddagger}$(RE)	ΔG_r	**13** (%)
7a	2-**N**C_5H_4	Me**S**CH_2	99.7	95.4	72.4	79
7b	2-**N**C_5H_4	Et**S**CH_2	97.4	83.8	83.0	64
7c	2-**N**C_5H_4	Pr**S**CH_2	101.3	88.2	84.1	79
7e	2-**N**C_5H_4	(*p*-MeC_6H_4)**S**CH_2	104.3	91.7	59.9	39
7f	2-**N**C_5H_4	(*p*-MeOC_6H_4)**S**CH_2	98.1	96.6	61.6	37
8b	2-**N**C_5H_4	Et_2**N**CH_2	129.1	112.0	88.3	98
9	2-**N**C_5H_4	(OC_4H_8)**N**CH_2	127.0	111.9	71.5	99
10	2-**N**C_5H_4	(C_6H_4)$_2$**P**O	95.7	73.0	148.5	94
11	2-**N**C_5H_4	(C_6H_4)$_2$**P**OCH_2	117.4	66.3	152.3	97
12	Me**S**C_6H_4	(^{i}Pr)$_2$**P**O	99.2*	55.4*	73.5*	85
14	Me_2**N**CH_2	Me_2**N**CH_2	-	-	-	98
15	Ph**S**CH_2	Ph**S**CH_2	-	-	-	47
16	+	+	-	-	-	57

* The ^{i}Pr groups in **12** were replaced with hydrogen (**12***) in the calculation.

+ Hermann-Beller complex (**16**) see **Fig. 6**.

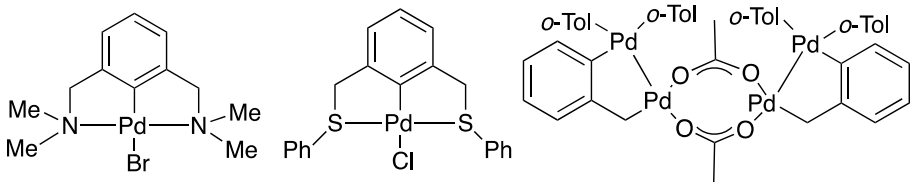

14 **15** **16**

Fig. 6. Palladacycles whose catalytic activity is compared with those of the unsymmetrical pincers investigated in the present study.

The PCS pincer palladacycle (**12***, with the ^{i}Pr groups replaced with H) has a similar overall reaction energy and transmetallation energy barrier to the SCN pincer palladacycles, and a slightly lower reductive elimination energy barrier than the NCP pincer palladacycles. It is possible that this model system **12*** predicts a slightly smaller activity than the intermediate catalytic activity observed for **12**.

3.3.2. Effect of substituents on the catalytic activity of the novel palladacycles

To determine the effect of the substituents on the thioether arm on the percentage (%) gas chromatographic (GC) conversions of the reactants during catalysis the application of **7a-c**, **7e** and **7f** in the SM reaction (**Table 3**) was considered. A summary of the results along with their TM and RE energy barriers and overall reaction energies (solvent corrected using *o*-xylene) are presented in **Table 3**. The results indicate that the palladacycles with alkyl substituted thioether side arms (**7a-c**) achieved higher % conversion of the reacting species than those with aryl substituted thioether side arms (**7e**,**f**), despite there being no discernible difference in the calculated rate-determining TM energy barrier or the RE energy barrier. However, there is a significant difference in the calculated overall reaction energies between **7a-c** (72 – 84 $kJmol^{-1}$) and **7e** and **7f** (59 – 62 $kJmol^{-1}$). The least endergonic and therefore, the most favorable for pre-catalyst activation were **7e** and **7f**. These also achieved the lower % conversions in comparison to **7a-c**.

In summary, the results presented in this section suggest that the ability to allow a slow, controlled release of the catalytically active Pd(0) is a possible way of improving the catalytic coupling in the SM reactions. This controlled release is facilitated by a high TM barrier (as in the case of the N'CN pincer palladacycles) or by a highly endergonic reaction energy (as in the case of the PCN pincer palladacycles). Facile formation of Pd(0) can lead to the formation of inactive palladium black [66]. The agglomeration of palladium nano-particles to form catalytically inactive palladium black is a key catalyst deactivation route [67,68]. Bedford *et al*., [19] also attributed higher catalyst activity to longevity of the pre-catalyst. The decreased catalytic activity by **7e** and **7f** can therefore, be explained by the relatively facile formation of Pd(0).

The data in **Table 3** also show that there is no significant difference in the catalytic activity of unsymmetrical and symmetrical pincer palladacycles. This may be because the *trans*-influence [30] and/or hemilability [69,70] of the pincer ligands (and complexes) do not affect the Pd-Cl and/or Pd-C bonds in the key TM and RE steps of the pre-catalyst activation for catalysis.

4. Conclusions

DFT has been used to elucidate the rational mechanistic approaches to Pd(0) generation from pincer palladacycles for catalysis in the SM cross-coupling reactions of aryl bromides and phenylboronic acid. It was found that the presence of the base in

the pre-catalyst activation is to significantly lower the activation energy barrier of the TM step and overall reaction energy of the process. In addition, solvent effects are dependent on the mechanism in question, with or without base. Furthermore, the slow, controlled release of the "true, active catalyst" for reaction in the SM coupling is more beneficial for the reaction and may be achieved either by a high activation energy barrier for the TM step, or overall reaction energy of the pre-catalyst activation process, or both. On this backdrop, a good pre-catalyst would be one that has donor atoms that provide the large TM, RE or overall reaction energies to control the release of catalytically active Pd(0) [9,19,57]. Finally, our investigations indicate that there is no significant difference in the catalytic activity of unsymmetrical and symmetrical pincer palladacycles in the SM couplings investigated.

5. Experimental Details

The solvents and chemicals used in this work were purchased from commercial suppliers and used without further purification, with reactions taking place open to atmosphere and moisture because of the air stability of the novel pre-catalysts. All NMR (^{1}H and ^{13}C) spectra were recorded on either a Varian 400 or 500 MHz spectrometer. GC measurements were obtained using a Perkin Elmer Auto-system XL Gas Chromatograph, utilizing a flame ionization detector, and a Supelco MDN-5S 30 m x 0.25 mm x 0.25 µm column, with a He mobile phase. HRMS of the products of the Suzuki-Miyaura catalysis was obtained using the EPSRC Mass Spectrometry Service at the University of Swansea.

5.1. Suzuki-Miyaura Catalytic Tests.

2-Bromomesitylene (1 mmol), 2-tolylboronic acid (1.5 mmol), K_2CO_3 (2 mmol) were added to a reaction vial and dissolved in *o*-xylene (3 cm^3). The 0.01 mol % solution of the tested novel pre-catalysts (**7a-c**, **7e**, **7f**, and **8b-12**) in CH_2Cl_2 was added, respectively. The reaction was heated at 130 $^{\circ}$C for 6 hours after which it was diluted with CH_2Cl_2 (20 cm^3), washed with H_2O (20 cm^3) and the organic layer was collected by passing over a hydrophobic frit. The solvent was removed *in vacuo* and the product obtained as a white solid in each case. ^{1}H NMR (500 MHz, Chloroform-*d*) δ 7.33 – 7.25 (m, 3H), 7.07 - 7.05 (m, 1H), 6.99 (s, 2H), 2.38 (s, 3H), 2.03 (s, 3H), 1.97 (s, 6H). ^{13}C NMR (100 MHz, Chloroform-*d*) δ 140.6, 138.2, 136.3, 135.9, 135.7, 129.9, 129.2 (2C), 128.0 (2C), 126.9, 126.0, 21.1, 20.2 (2C), 19.5. HRMS (m/z). Calculated for $[C_{16}H_{18}]^{+}$ 210.1409. Found 210.1416.

Appendix A. Supplementary Information

The detailed mechanisms, Gibbs free energy profiles, and tabulated energetic data with and without solvent corrections are provided in the Supplementary Information. Also included is the QTAIM molecular graph of **Int1** for the symmetrical pincer palladacycles **1**-**3** and the Cartesian coordinates for all the structures.

Author Information

Corresponding Author(s)

*E-mail: h.cox@sussex.ac.uk; j.spencer@sussex.ac.uk.

Notes

The authors declare that there are no competing interests.

Acknowledgments

We would like to thank the Royal Thai Government, the University of Sussex and the Tertiary Education Trust Fund of Nigeria for fully funded PhD scholarships (SB, GWR and MT, respectively). We would like to acknowledge Christopher Dadswell for his support and use of the GC equipment and Johnson Matthey for the loan of palladium salts. We would also like to thank the EPSRC Mass Spectrometry Facility (Swansea University). Finally, we would like to acknowledge the use of the EPSRC UK National Service for Computational Chemistry Software (NSCCS) at Imperial College London in performing part of this work.

Dedication. To Gerard van Koten for his seminal contributions to pincer chemistry.

References

[1] J. Dupont, C.S. Consorti, J. Spencer, The Potential of Palladacycles: More Than Just Precatalysts, Chem. Rev. 105 (2005) 2527–2572. doi:10.1021/cr030681r.

[2] J. Dupont, M. Pfeffer, J. Spencer, Palladacycles − An Old Organometallic Family Revisited: New, Simple, and Efficient Catalyst Precursors for Homogeneous Catalysis, Eur. J. Inorg. Chem. 2001 (2001) 1917–1927. doi:10.1002/1099-0682(200108)2001:8<1917::AID-EJIC1917>3.0.CO;2-M.

[3] R.B. Bedford, Palladacyclic catalysts in C–C and C–heteroatom bond-forming reactions, Chem. Commun. (2003) 1787–1796. doi:10.1039/B211298C.

[4] R. Ratti, Palladacycles - Versatile Catalysts for Carbon-Carbon Coupling Reactions, Can. Chem. Trans. 2 (2014) 467–488. doi:10.13179/canchemtrans.2014.02.04.0128.

[5] W.A. Herrmann, C. Brossmer, K. Öfele, C.-P. Reisinger, T. Priermeier, M. Beller, H. Fischer, Palladacycles as Structurally Defined Catalysts for the Heck

Olefination of Chloro- and Bromoarenes, Angew. Chemie Int. Ed. English. 34 (1995) 1844–1848. doi:10.1002/anie.199518441.
[6] M. Beller, H. Fischer, W.A. Herrmann, K. Öfele, C. Brossmer, Palladacycles as Efficient Catalysts for Aryl Coupling Reactions, Angew. Chemie Int. Ed. English. 34 (1995) 1848–1849. doi:10.1002/anie.199518481.
[7] J. Dupont, M. Pfeffer, Palladacycles, Wiley-VCH Verlag GmbH & Co. KGaA, Weinheim, Germany, 2008.
[8] N. Selander, K. J. Szabó, Catalysis by Palladium Pincer Complexes, Chem. Rev. 111 (2011) 2048–2076. doi:10.1021/cr1002112.
[9] S. Boonseng, G.W. Roffe, J. Spencer, H. Cox, The nature of the bonding in symmetrical pincer palladacycles, Dalton Trans. 44 (2015) 7570–7577. doi:10.1039/C5DT00031A.
[10] K.J. Szabó, O.F. Wendt, eds., Pincer and Pincer-Type Complexes, Wiley-VCH Verlag GmbH & Co. KGaA, Weinheim, Germany, 2014.
[11] D. Morales-Morales, C.M. Jensen, eds., The Chemistry of Pincer Compounds, Elsevier, Amsterdam, 2007.
[12] N. Miyaura, K. Yamada, A. Suzuki, A new stereospecific cross-coupling by the palladium-catalyzed reaction of 1-alkenylboranes with 1-alkenyl or 1-alkynyl halides, Tetrahedron Lett. 20 (1979) 3437–3440. doi:10.1016/S0040-4039(01)95429-2.
[13] I. Moreno, R. SanMartin, B. Ines, M.T. Herrero, E. Domínguez, Recent advances in the use of unsymmetrical palladium pincer complexes, Curr. Org. Chem. 13 (2009) 878–895. doi:10.2174/138527209788452144.
[14] R.F. Heck, J.P. Nolley, Palladium-catalyzed vinylic hydrogen substitution reactions with aryl, benzyl, and styryl halides, J. Org. Chem. 37 (1972) 2320–2322. doi:10.1021/jo00979a024.
[15] M. Gagliardo, N. Selander, N.C. Mehendale, G. Van Koten, R.J.M. Klein Gebbink, K.J. Szabó, Catalytic performance of symmetrical and unsymmetrical sulfur-containing pincer complexes: Synthesis and tandem catalytic activity of the first PCS-pincer palladium complex, Chem. - A Eur. J. 14 (2008) 4800–4809. doi:10.1002/chem.200800350.
[16] B.-S. Zhang, C. Wang, J.-F. Gong, M.-P. Song, Facile synthesis of achiral and chiral PCN pincer palladium(II) complexes and their application in the Suzuki and copper-free Sonogashira cross-coupling reactions, J. Organomet. Chem. 694 (2009) 2555–2561. doi:10.1016/j.jorganchem.2009.04.002.
[17] J. Louie, J.F. Hartwig, A Route to Pdo from PdII Metallacycles in Animation and Cross-Coupling Chemistry, Angew. Chemie Int. Ed. English. 35 (1996) 2359–2361. doi:10.1002/anie.199623591.
[18] R.B. Bedford, S.L. Welch, Palladacyclic phosphinite complexes as extremely high activity catalysts in the Suzuki reaction, Chem. Commun. 2 (2001) 129–130. doi:10.1039/b008470k.
[19] R.B. Bedford, S.L. Hazelwood, P.N. Horton, M.B. Hursthouse, Orthopalladated phosphinite complexes as high-activity catalysts for the Suzuki reaction, Dalton Trans. 2 (2003) 4164–4174. doi:10.1039/b303657j.
[20] F. d'Orlyé, A. Jutand, In situ formation of palladium(0) from a P,C-palladacycle, Tetrahedron. 61 (2005) 9670–9678. doi:10.1016/j.tet.2005.07.098.
[21] J. Spencer, D.P. Sharratt, J. Dupont, A.L. Monteiro, V.I. Reis, M.P. Stracke, F. Rominger, I.M. McDonald, Synthesis and evaluation of 5-phenyl-1H-1,4-benzodiazepin-2(3H)-one-based palladium complexes as precatalysts in C−C

bond forming reactions, Organometallics. 24 (2005) 5665–5672. doi:10.1021/om0506623.
[22] V.A. Kozlov, D. V. Aleksanyan, Y. V. Nelyubina, K.A. Lyssenko, P. V. Petrovskii, A.A. Vasil'ev, I.L. Odinets, Hybrid thiophosphoryl-benzothiazole palladium SCN-pincer complexes: Synthesis and effect of structure modifications on catalytic performance in the suzuki cross-coupling, Organometallics. 30 (2011) 2920–2932. doi:10.1021/om101012r.
[23] D. V Aleksanyan, V.A. Kozlov, N.E. Shevchenko, V.G. Nenajdenko, A.A. Vasil'ev, Y. V Nelyubina, I. V Ananyev, P. V Petrovskii, I.L. Odinets, Hybrid NCS palladium pincer complexes of thiophosphorylated benzaldimines and their ketimine analogs, J. Organomet. Chem. 711 (2012) 52–61. doi:10.1016/j.jorganchem.2012.03.029.
[24] M. García-Melchor, A.A.C. Braga, A. Lledós, G. Ujaque, F. Maseras, Computational Perspective on Pd-Catalyzed C–C Cross-Coupling Reaction Mechanisms, Acc. Chem. Res. 46 (2013) 2626–2634. doi:10.1021/ar400080r.
[25] J. Dupont, M. Pfeffer, Reactions of cyclopalladated compounds. Part 24. Reactivity of the Pd–C bond of cyclopalladated compounds towards isocyanides and carbon monoxide. Role of the donor group, J. Chem. Soc., Dalt. Trans. (1990) 3193–3198. doi:10.1039/DT9900003193.
[26] J. Dupont, N. Beydoun, M. Pfeffer, Reactions of cyclopalladated compounds. Part 21. Various examples of sulphur-assisted intramolecular palladation of aryl and alkyl groups, J. Chem. Soc. Dalt. Trans. (1989) 1715. doi:10.1039/dt9890001715.
[27] C.A. Kruithof, H.P. Dijkstra, M. Lutz, A.L. Spek, R.J.M.K. Gebbink, G. van Koten, X-Ray and NMR Study of the Structural Features of SCS-Pincer Metal Complexes of the Group 10 Triad, Organometallics. 27 (2008) 4928–4937. doi:10.1021/om800324w.
[28] B.-B. Liu, X.-R. Wang, Z.-F. Guo, Z.-L. Lu, Mononuclear versus dinuclear palladacycles derived from 1,3-bis(N,N-dimethylaminomethyl)benzene: Structures and catalytic activity, Inorg. Chem. Commun. 13 (2010) 814–817. doi:10.1016/j.inoche.2010.03.035.
[29] G.W. Roffe, S. Boonseng, C.B. Baltus, S.J. Coles, I.J. Day, R.N. Jones, N.J. Press, M. Ruiz, G.J. Tizzard, H. Cox, J. Spencer, A synthetic, catalytic and theoretical investigation of an unsymmetrical SCN pincer palladacycle, R. Soc. Open Sci. 3 (2016) 150656. doi:10.1098/rsos.150656.
[30] S. Boonseng, G. Roffe, R. Jones, G. Tizzard, S. Coles, J. Spencer, H. Cox, The Trans Influence in Unsymmetrical Pincer Palladacycles: An Experimental and Computational Study, Inorganics. 4 (2016) 25. doi:10.3390/inorganics4030025.
[31] G.W. Roffe, G.J. Tizzard, S.J. Coles, H. Cox, J. Spencer, Synthesis of unsymmetrical NCN′ and PCN pincer palladacycles and their catalytic evaluation compared with a related SCN pincer palladacycle, Org. Chem. Front. 3 (2016) 957–965. doi:10.1039/C6QO00198J.
[32] M.J. Frisch, G.W. Trucks, H.B. Schlegel, G.E. Scuseria, M.A. Robb, J.R. Cheeseman, G. Scalmani, V. Barone, B. Mennucci, G.A. Petersson, H. Nakasuji, M. Caricato, X. Li, H.P. Hratchian, A.F. Izmaylov, J. Bloino, G. Zheng, J.L. Sonnenberg, M. Hada, M. Ehara, K. Toyota, R. Fukuda, J. Hasegawa, M. Ishida, T. Nakajima, Y. Honda, O. Kitao, H. Nakai, T. Vreven, J.A.J. Montgomery, J.E. Peralta, F. Ogliaro, M. Bearpark, J.J. Heyd, E. Brothers, K.N. Kudin, V.N. Staroverov, T. Keith, R. Kobayashi, J. Normand, K. Raghavachari, A. Rendell, J.C. Burant, S.S. Iyengar, J. Tomasi, M. Cossi,

N. Rega, J.M. Millam, M. Klene, J.E. Knox, J.B. Cross, V. Bakken, C. Adamo, J. Jaramillo, R. Gomperts, R.E. Stratmann, O. Yazyev, A.J. Austin, R. Cammi, C. Pomelli, J.W. Ochterski, R.L. Martin, K. Morokuma, V.G. Zakrzewski, G.A. Voth, P. Salvador, J.J. Dannenberg, S. Dapprich, A.D. Daniels, O. Farkas, J.B. Foresman, J. V Ortiz, J. Cioslowski, D.J. Fox, Gaussian 09, Revision D.01, Gaussian, Inc., Wallingford CT, (2013).

[33] J.P. Perdew, K. Burke, M. Ernzerhof, Generalized Gradient Approximation Made Simple, Phys. Rev. Lett. 77 (1996) 3865–3868. doi:10.1103/PhysRevLett.77.3865.

[34] J.P. Perdew, K. Burke, M. Ernzerhof, Generalized Gradient Approximation Made Simple, Phys. Rev. Lett. 78 (1997) 1396–1396.

[35] J.P. Perdew, K. Burke, M. Ernzerhof, Perdew, Burke, and Ernzerhof Reply:, Phys. Rev. Lett. 80 (1998) 891–891. doi:10.1103/PhysRevLett.80.891.

[36] J. Chai, M. Head-Gordon, Long-range corrected hybrid density functionals with damped atom–atom dispersion corrections, Phys. Chem. Chem. Phys. 10 (2008) 6615. doi:10.1039/b810189b.

[37] Y. Zhao, D.G. Truhlar, Density functional theory for reaction energies: Test of meta and hybrid meta functionals, range-separated functionals, and other high-performance functionals, J. Chem. Theory Comput. 7 (2011) 669–676. doi:10.1021/ct1006604.

[38] M. Dolg, U. Wedig, H. Stoll, H. Preuss, Energy-adjusted ab initio pseudopotentials for the first row transition elements, J. Chem. Phys. 86 (1987) 866. doi:10.1063/1.452288.

[39] D. Andrae, U. Häußermann, M. Dolg, H. Stoll, H. Preuß, Energy-adjusted ab initio pseudopotentials for the second and third row transition elements, Theor. Chim. Acta. 77 (1990) 123–141. doi:10.1007/BF01114537.

[40] H.B. Schlegel, Optimization of equilibrium geometries and transition structures, J. Comput. Chem. 3 (1982) 214–218. doi:10.1002/jcc.540030212.

[41] K. Fukui, Formulation of the reaction coordinate, J. Phys. Chem. 74 (1970) 4161–4163. doi:10.1021/j100717a029.

[42] K. Fukui, The path of chemical reactions - the IRC approach, Acc. Chem. Res. 14 (1981) 363–368. doi:10.1021/ar00072a001.

[43] C. Gonzalez, H.B. Schlegel, Reaction path following in mass-weighted internal coordinates, J. Phys. Chem. 94 (1990) 5523–5527. doi:10.1021/j100377a021.

[44] S. Miertuš, E. Scrocco, J. Tomasi, Electrostatic interaction of a solute with a continuum. A direct utilizaion of AB initio molecular potentials for the prevision of solvent effects, Chem. Phys. 55 (1981) 117–129. doi:10.1016/0301-0104(81)85090-2.

[45] J. Tomasi, B. Mennucci, R. Cammi, Quantum Mechanical Continuum Solvation Models, Chem. Rev. 105 (2005) 2999–3094. doi:10.1021/cr9904009.

[46] G. Scalmani, M.J. Frisch, Continuous surface charge polarizable continuum models of solvation. I. General formalism, J. Chem. Phys. 132 (2010) 114110. doi:10.1063/1.3359469.

[47] R.F.W. Bader, Atoms in Molecules, Acc. Chem. Res. 18 (1985) 9–15.

[48] T. Lu, F. Chen, Multiwfn: A multifunctional wavefunction analyzer, J. Comput. Chem. 33 (2012) 580–592. doi:10.1002/jcc.22885.

[49] C. Sosa, J. Andzelm, B.C. Elkin, E. Wimmer, K.D. Dobbs, D.A. Dixon, A local density functional study of the structure and vibrational frequencies of molecular transition-metal compounds, J. Phys. Chem. 96 (1992) 6630–6636. doi:10.1021/j100195a022.

[50] A.R. Kapdi, G. Dhangar, J.L. Serrano, J. Pérez, L. García, I.J.S. Fairlamb, [Pd(C^N)(X)(PPh_3)] palladacycles react with 2,4,6-trifluorophenyl boronic acid to give stable transmetallation products of the type [Pd(C^N)(2,4,6-F_3 C_6 H_2)(PPh_3)]†, Chem. Commun. 50 (2014) 9859. doi:10.1039/C4CC04203D.
[51] C.A. Hunter, J.K.M. Sanders, The nature of π-π interactions, J. Am. Chem. Soc. 112 (1990) 5525–5534. doi:10.1021/ja00170a016.
[52] M.O. Sinnokrot, C.D. Sherrill, Substituent effects in π-π interactions: Sandwich and t-shaped configurations, J. Am. Chem. Soc. 126 (2004) 7690–7697. doi:10.1021/ja049434a.
[53] E. Arunan, G.R. Desiraju, R. a. Klein, J. Sadlej, S. Scheiner, I. Alkorta, D.C. Clary, R.H. Crabtree, J.J. Dannenberg, P. Hobza, H.G. Kjaergaard, A.C. Legon, B. Mennucci, D.J. Nesbitt, Definition of the hydrogen bond (IUPAC Recommendations 2011), Pure Appl. Chem. 83 (2011) 1637–1641. doi:10.1351/PAC-REC-10-01-02.
[54] K. Matos, J.A. Soderquist, Alkylboranes in the Suzuki−Miyaura Coupling: Stereochemical and Mechanistic Studies, J. Org. Chem. 63 (1998) 461–470. doi:10.1021/jo971681s.
[55] H. Lakmini, I. Ciofini, A. Jutand, C. Amatore, C. Adamo, Pd-catalyzed homocoupling reaction of arylboronic acid: Insights from density functional theory, J. Phys. Chem. A. 112 (2008) 12896–12903. doi:10.1021/jp801948u.
[56] A.A.C. Braga, N.H. Morgon, G. Ujaque, A. Lledós, F. Maseras, Computational study of the transmetalation process in the Suzuki–Miyaura cross-coupling of aryls, J. Organomet. Chem. 691 (2006) 4459–4466. doi:10.1016/j.jorganchem.2006.02.015.
[57] A.G. Orpen, N.G. Connelly, Structural systematics: the role of P-A σ* orbitals in metal-phosphorus π-bonding in redox-related pairs of M-PA3 complexes (A = R, Ar, OR; R = alkyl), Organometallics. 9 (1990) 1206–1210. doi:10.1021/om00118a048.
[58] P.K. Sajith, C.H. Suresh, Mechanisms of Reductive Eliminations in Square Planar Pd(II) Complexes: Nature of Eliminated Bonds and Role of trans Influence, Inorg. Chem. 50 (2011) 8085–8093. doi:10.1021/ic2004563.
[59] L. Estévez, L.W. Tuxworth, J. Sotiropoulos, P.W. Dyer, K. Miqueu, Combined DFT and experimental studies of C–C and C–X elimination reactions promoted by a chelating phosphine–alkene ligand: the key role of penta-coordinate PdII, Dalton Trans. 43 (2014) 11165. doi:10.1039/c4dt00340c.
[60] H. Ossor, M. Pfeffer, J.T.B.H. Jastrzebski, C.H. Stam, Reactivity of cycopalladated compounds. 14. Alkyne insertion into the palladium-carbon bond of a metallacycle stabilized by a weak oxygen→palladium bond leading to an unusual (η2-aryl)→palladium interaction. Molecular structure of [NC, Inorg. Chem. 26 (1987) 1169–1171. doi:10.1021/ic00254a037.
[61] A.A.C. Braga, N.H. Morgon, G. Ujaque, F. Maseras, Computational characterization of the role of the base in the Suzuki-Miyaura cross-coupling reaction, J. Am. Chem. Soc. 127 (2005) 9298–9307. doi:10.1021/ja050583i.
[62] C. Sicre, A.A.C. Braga, F. Maseras, M.M. Cid, Mechanistic insights into the transmetalation step of a Suzuki-Miyaura reaction of 2(4)-bromopyridines: characterization of an intermediate, Tetrahedron. 64 (2008) 7437–7443. doi:10.1016/j.tet.2008.05.018.
[63] M. Pérez-Rodríguez, A.A.C. Braga, M. Garcia-Melchor, M.H. Pérez-Temprano, J.A. Casares, G. Ujaque, A.R. de Lera, R. Álvarez, F. Maseras, P.

Espinet, C−C Reductive Elimination in Palladium Complexes, and the Role of Coupling Additives. A DFT Study Supported by Experiment, J. Am. Chem. Soc. 131 (2009) 3650–3657. doi:10.1021/ja808036j.
[64] M. Pérez-Rodríguez, A.A.C. Braga, A.R. de Lera, F. Maseras, R. Álvarez, P. Espinet, A DFT Study of the Effect of the Ligands in the Reductive Elimination from Palladium Bis(allyl) Complexes †, Organometallics. 29 (2010) 4983–4991. doi:10.1021/om1001974.
[65] D.M. Grove, G. Van Koten, J.N. Louwen, J.G. Noltes, A.L. Spek, H.J.C. Ubbels, Trans-2,6-bis[(dimethylamino)methyl]phenyl-N,N',C complexes of palladium(II) and platinum(II). Crystal structure of [PtI[MeC6H3(CH2NMe2)2-o,o']]BF4: a cyclohexadienyl carbonium ion with a σ-bonded metal substituent, J. Am. Chem. Soc. 104 (1982) 6609–6616. doi:10.1021/ja00388a022.
[66] G. van Koten, Organometallic Pincer Chemistry, Springer Berlin Heidelberg, Berlin, Heidelberg, 2013. doi:10.1007/978-3-642-31081-2.
[67] A.H.M. de Vries, J.M.C.A. Mulders, J.H.M. Mommers, H.J.W. Henderickx, J.G. de Vries, Homeopathic Ligand-Free Palladium as a Catalyst in the Heck Reaction. A Comparison with a Palladacycle, Org. Lett. 5 (2003) 3285–3288. doi:10.1021/ol035184b.
[68] J.G. de Vries, A unifying mechanism for all high-temperature Heck reactions. The role of palladium colloids and anionic species, Dalton Trans. (2006) 421–429. doi:10.1039/B506276B.
[69] P. Braunstein, F. Naud, Hemilability of Hybrid Ligands and the Coordination Chemistry of Oxazoline-Based Systems, Angew. Chemie Int. Ed. 40 (2001) 680–699. doi:10.1002/1521-3773(20010216)40:4<680::AID-ANIE6800>3.0.CO;2-0.
[70] A. Fleckhaus, A.H. Mousa, N.S. Lawal, N.K. Kazemifar, O.F. Wendt, Aromatic PCN palladium pincer complexes. Probing the hemilability through reactions with nucleophiles, Organometallics. 34 (2015) 1627–1634. doi:10.1021/om501231k.